Modification of the Structure, Phase Composition, and Mechanical Properties of the Ti–C_{60}–Ti Films Implanted with Boron Ions

L. V. Baran*

Belarusian State University, Minsk, 220030 Belarus

**e-mail: baran@bsu.by*

Abstract—Changes in the structure, phase composition, and mechanical properties of Ti–C_{60}–Ti films implanted with B^+ ions (E = 80 keV, $D = 1 \times 10^{16}$ ions/cm^2) after annealing in vacuum at a temperature of 570 K (3 h) are studied by atomic force microscopy, X-ray diffraction, and nanoindentation. The films are synthesized by resistive evaporation in vacuum. Titanium and C_{60} fullerite layers are sequentially deposited onto a substrate of oxidized single crystal silicon. It is established that intense diffusion of titanium into the fullerite layer occurs during the condensation of the fullerite layer (h = 250 nm) on the underlying titanium layer (h = 120 nm) and then the titanium layer (h = 150 nm) on the fullerite layer. Implantation of titanium–fullerite–titanium films with boron ions leads to mixing of titanium and fullerite layers, while the size of structural components increases from 40 nm to 80 nm compared to nonimplanted films. Auger electron spectroscopy reveals that ion implantation gives rise to an increase in the atomic fraction of oxygen in the films and the formation of a new phase of $Ti_xO_yC_{60}$, which leads to an increase in the nanohardness of the mixed layers. The implanted Ti–C_{60}–Ti films are annealed in vacuum at T = 570 K for t = 3 h. Thermal annealing gives rise to recrystallization of the fullerite phase and intense growth of a new phase of $Ti_xO_yC_{60}$ with improved mechanical properties.

Keywords: fullerite–titanium films, ion implantation, structure, phase composition, mechanical properties, atomic force microscopy

DOI: 10.1134/S207511332303005X

INTRODUCTION

The synthesis of new materials based on fullerite, which is an allotropic phase of carbon, and transition metal titanium is a promising field of research, since titanium and its compounds are widely used in various fields of science and technology, including biomedicine [1–13]. It has been established that new phases in the C_{60}–Ti system are formed both at the stage of film deposition and during subsequent thermal treatment of the samples. In [4], a new phase of $Ti_{5.3}C_{60}$ was synthesized by deposition of fullerite–titanium films in ultrahigh vacuum from a combined atomic–molecular f low. The simulation of X-ray emission spectra of codeposited fullerite–titanium films carried out in [5] showed the possibility of chemical bonding between titanium atoms and fullerene molecules through a six-membered C_{60} ring. The Raman spectra of the C_{60}–Ti films synthesized in [6] also indicate the presence of a chemical bond between Ti and C_{60}.

Ion implantation is a method for the synthesis of new phases in thin film structures. However, the interaction of accelerated charged ions with fullerene molecules can lead to their destruction. Thus, the breakage of conjugated π bonds and the destruction of the C_{60} structure up to the decay of molecules into small carbon fragments that do not have conjugated π bonds but contain the broken and sp^2 hybrid bonds were established when studying the C_{60} samples in the shape of a film with a thickness of 400 nm on a Si substrate before and after exposure to argon ions with E = 1–4 keV under currents of 0.4 and 20 μA [14]. Fullerene molecules are also partially destroyed as a result of ion implantation [15–18]. However, if fullerite is implanted with ions through a metal layer, then ions that lose energy do not destroy fullerene molecules, and the energy released in the collision cascade promotes a solid phase reaction of metal atoms and fullerene molecules at the layer interface [19].

The aim of this study was to analyze changes in the structure, phase composition, and mechanical properties of titanium–fullerite films implanted with boron ions and then subjected to thermal annealing in vacuum.

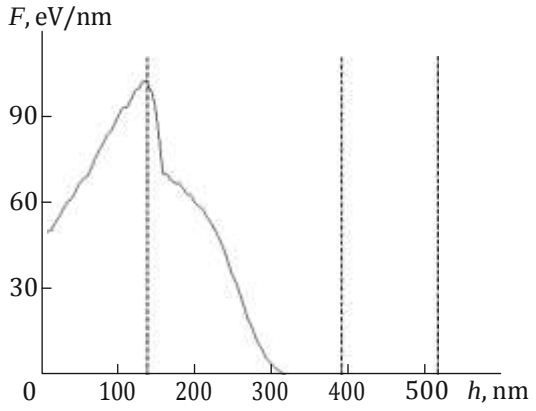

Fig. 1. Depth distribution profile of the energy released in elastic collisions of Ti–C_{60}–Ti (150–250–120 nm) films with boron ions.

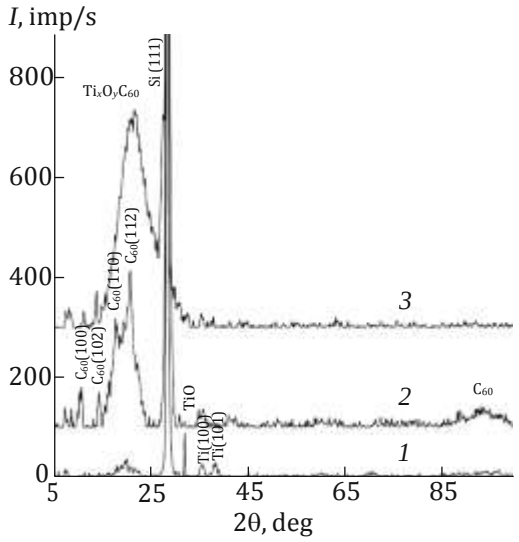

Fig. 2. X-ray diffraction patterns of Ti–C_{60}–Ti films (*1*) before ion implantation, (*2*) after implantation with boron ions (E = 80 keV, $D = 1 \times 10^{16}$ ions/cm^2), and (*3*) after annealing the films implanted with boron ions at 570 K for 3 h.

EXPERIMENTAL

Layers of metal and fullerite were sequentially deposited onto an unheated oxidized single-crystal silicon wafer with the (111) surface orientation in a VUP-5M device using titanium of VT1-0 grade and C_{60} powder of 99.9% purity. Three-layer Ti–C_{60}–Ti films with layer thicknesses of 150, 250, and 120 nm were obtained. The samples were irradiated with boron ions with an energy of E = 80 keV. The implantation dose was 1×10^{16} ions/cm^2, and the ion current density was 3.5 μA/cm^2.

The layer thickness was chosen in such a way that the maximum amount of defects by implantation were created at the interface between the titanium and fullerite layers on the side of implantation, and the ions did not reach the far C_{60}–Ti interface. Figure 1 shows the results of calculating the defect distribution profile in an implanted layered structure using the SRIM software package [20]. On the basis of calculation, the implanted ions will experience the maximum energy loss near the interface between the upper titanium film and fullerite. With such a scheme of the experiment, the far interface can serve as a reference for the analysis of diffusion processes occurring at the nearest interface as a result of a cascade of collisions caused by accelerated ions when they penetrate into the film.

The films were annealed in a fast-response vacuum furnace at a temperature of 570 K for 3 h. The surface morphology of the films was studied by atomic force microscopy on a Solver P47 Pro scanning probe microscope operated in the amplitude modulation mode. We used super-sharp silicon probes with a tip curvature radius of less than 3 nm. The distribution of local stiffness was studied by the force modulation method; a detailed technique is described in [19]. The elemental composition was analyzed using a PHI-660 scanning Auger electron spectrometer (PerkinElmer). Atoms were excited by an electron beam with an electron energy of 3 keV.

The film was sputtered using Ar^+ ions with an energy of 3.5 keV. The X-ray diffraction studies were performed on a DRON-4.13 diffractometer with CuK_α radiation. The dynamic hardness measurements were performed on a SHIMADZU DUH202 ultramicrohardness tester with a trihedral Berkovich indenter in accordance with the measurement procedure described in [21].

RESULTS AND DISCUSSION

It is established by the X-ray diffraction method that a nanocrystalline fullerite structure and a subcrystalline structure of the α-modification of titanium are formed during condensation on a substrate of oxidized single-crystal silicon indexed in the hexagonal syngony (Fig. 2). The diffraction pattern also contains an intense line of titanium monoxide, the presence of which in the samples may be due to the sorption properties of titanium. The titanium film has a nanocrystalline structure with an average lateral size of structural components of 40 nm (Fig. 3a), while the root mean square (RMS) roughness of the film does not exceed 3.5 nm.

Implantation of titanium–fullerite films with boron ions leads to substantial changes in the structure and phase. An analysis of the film morphology showed that the lateral size of the structural components increased to 60–80 nm at an RMS roughness of 6.0 nm (Fig. 3b). The intensity of reflections of the

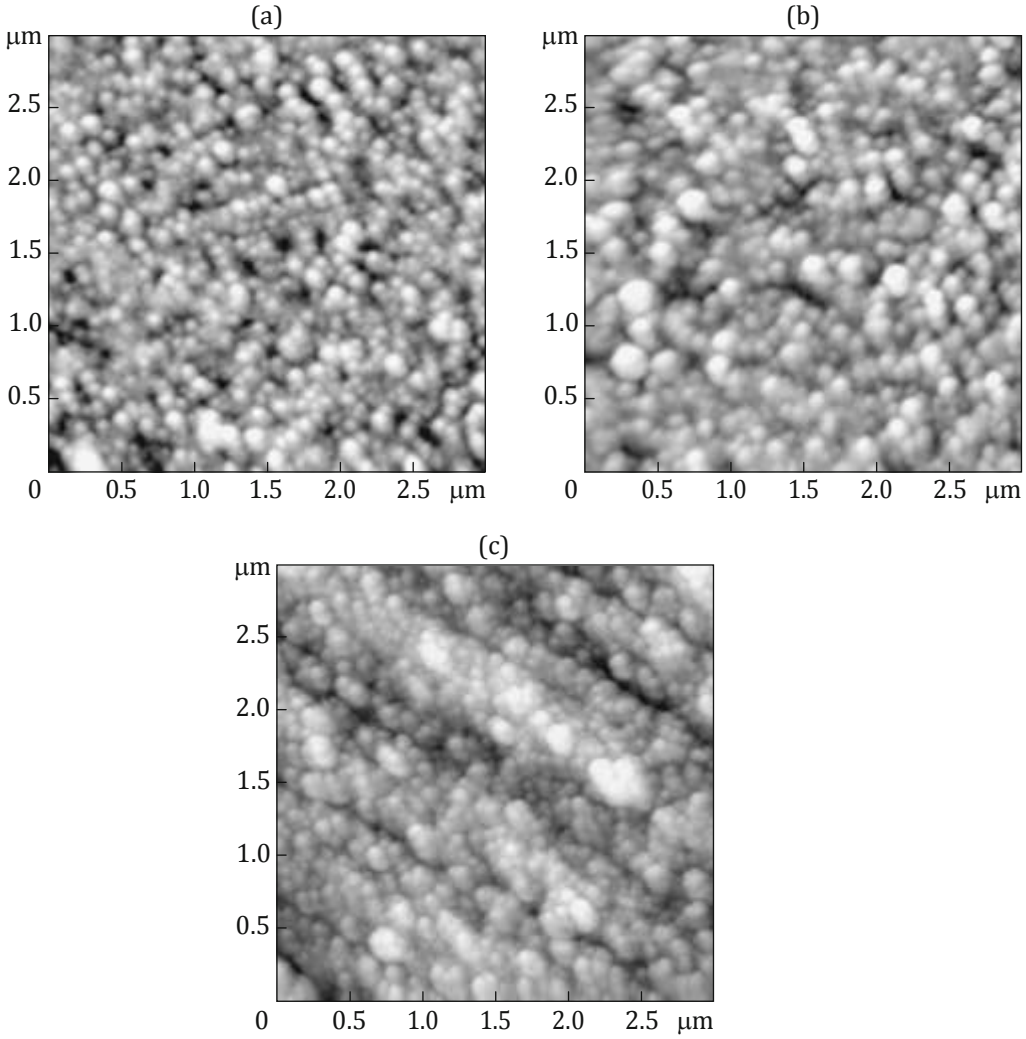

Fig. 3. Atomic force microscopy images of Ti–C_{60}–Ti films (a) before ion implantation, (b) after implantation with boron ions (E = 80 keV, $D = 1 \times 10^{16}$ ions/cm^2), and (c) after annealing the films implanted with boron ions at 570 K for 3 h.

fullerite phase in the X-ray diffraction pattern of the implanted sample increases by a factor of almost 10, and a number of new lower intensity lines appear (see Fig. 2, curve *2*). A sharp increase in the intensity of X-ray reflections may indicate the occurrence of recrystallization processes in the fullerite phase, and the appearance of new diffraction maxima may indicate the formation of a new phase.

The intensity of the Ti(002) line in the sample implanted with B^+ ions decreases, which can be explained by radiation accelerated diffusion of titanium atoms into the fullerite matrix. The line of the TiO(102) phase, which was present in the X-ray diffraction pattern of the nonimplanted sample, also disappears.

The Auger spectroscopy studies showed that the oxygen concentration in implanted films increases compared to nonimplanted samples (Fig. 4). In freshly prepared films, oxygen with a maximum concentration of 20 at % is present at the interface between the titanium and fullerite layers. In the lower titanium layer, the oxygen concentration does not exceed 7 at %. The oxygen content in the upper Ti layer is noticeably higher and monotonically increases upon approaching the surface from 6 at % in the deep part of the film to 60 at % on the surface.

Such a behavior of the distribution of chemical elements can be caused by two circumstances: the reduced density of the deposited titanium layer compared to the bulk material and the storage of samples in air. The increased oxygen content at the far C_{60}–Ti interface is due to the sorption of oxygen by micropores when they are in contact with the atmosphere before deposition of the second layer. The oxygen content in the fullerite film is 1 at %, and the same amount was found in the titanium layer. This fact suggests that titanium monoxide is dissolved in the fullerite matrix.

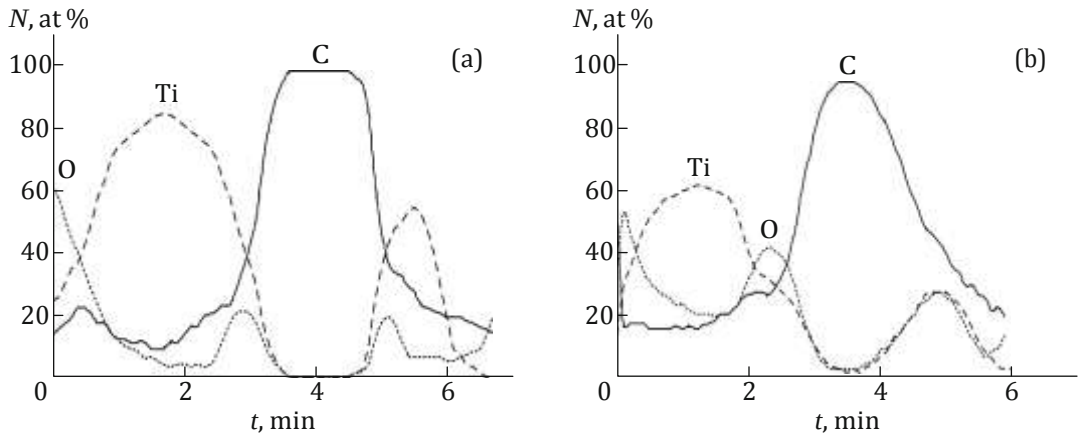

Fig. 4. Distribution profiles of elements over the thickness of Ti–C_{60}–Ti films (a) before ion implantation and (b) after implantation with boron ions (E = 80 keV, $D = 1 \times 10^{16}$ ions/cm^2).

The distribution of carbon in freshly prepared films has a trapezoidal shape with a maximum concentration at the level of 98%. A small part of carbon lies at the interface between the films and creates a transition layer, which indicates the mixing of titanium atoms and fullerene molecules already at the stage of sample preparation.

The Auger spectroscopy method revealed that the carbon content in the upper titanium film increases after ion implantation (Fig. 4b), which can be explained by radiation accelerated diffusion and mixing of layers during implantation. After implantation, the thickness of the transition layer at the near the Ti–C_{60} interface doubles, and shelves are observed in the distribution curves of the atomic concentrations at the levels of 30 at % for C and 35 at % for Ti, which indicates the formation of a new phase. The reaction between titanium atoms and fullerene molecules with the formation of a new phase of Ti_xC_{60} was also established in [5, 11, 22, 23].

Boron was not detected by Auger spectroscopy, since its concentration with a given implantation dose (1×10^{16} ions/cm^2) is 1 at % on average, which is comparable to the measurement error for light elements. Under certain conditions, boron can be involved in a chemical reaction with the atoms of the matrix. However, the concentration of implanted ions is not sufficient for the formation of chemical compounds evenly distributed over the entire implanted layer under the given implantation conditions, since it does not meet the required stoichiometric proportions. In principle, this does not exclude the possibility of formation of chemical compounds of implanted atoms in some local regions of the matrix, the small sizes of which make their detection impossible by the X-ray diffraction method.

After ion implantation, the atomic fraction of oxygen doubles over the entire depth of the upper titanium film owing to a low vacuum in the accelerator chamber and an increase in the temperature during implantation. As is well known, titanium is covered with a passivating film of TiO_2 oxide at room temperature. In the ion implantation process, a part of the oxide gets deep into the film as a result of a cascade of collisions. The defects created by ion implantation also facilitate the penetration of oxygen atoms into the titanium film. The crystallite size of the film is less than 100 nm, so the proportion of defective interfaces along which oxygen diffusion can also occur is very high. Moreover, ascending diffusion is observed in the region of the interface, in which the maximum amount of radiation defects is located.

The content of oxygen and titanium in the fullerite film increases to 3–4 at %. The disappearance of the titanium oxide lines in the X-ray diffraction pattern of the implanted film is probably associated with the formation of a new phase of $Ti_xO_yC_{60}$. In [4], the formation of the $Ti_xO_yC_{60}$ phase was also established by X-ray photoelectron spectroscopy and Raman spectroscopy.

Figure 5 shows the dependence of the dynamic hardness of the films on the penetration depth of the indenter. The observed decrease in the nanohardness of nonimplanted films with depth is due to the low mechanical characteristics of the fullerite layer located under the titanium film (the microhardness value is 145 MPa for a fullerite single crystal [24] and 240 MPa for a fullerite film deposited on a glass substrate [25]). Ion implantation leads to strengthening of the region at a depth of 150–200 nm as a result of the mixing of titanium and fullerite layers and the formation of new phases.

After thermal annealing in vacuum at 570 K (3 h), the nanocrystalline structure of the implanted titanium–fullerite–titanium films is preserved, and the size of the structural components slightly increases to

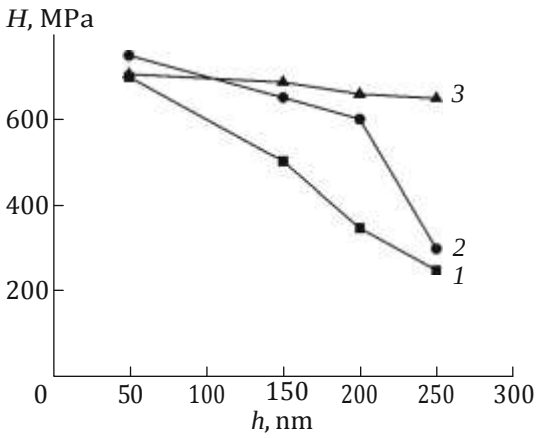

Fig. 5. Dependences of the dynamic hardness on the depth of indenter penetration for Ti–C_{60}–Ti films (*1*) before implantation, (*2*) after implantation with boron ions (E = 80 keV, $D = 1 \times 10^{16}$ ions/cm^2), and (*3*) after annealing the films implanted with boron ions at 570 K for 3 h.

90 nm (Fig. 3c), which is associated with the occurrence of recrystallization processes.

The phase composition of the samples also changes substantially after annealing. The X-ray diffraction pattern of the annealed samples shows an intense halo in the region of small angles (see Fig. 2, curve *3*), while the (100) and (101) lines of titanium and the halo in the region of angles of 2θ = 85°–99°, which were present in the spectrum of implanted samples before annealing (see Fig. 2, curve *2*), disappear.

The increase in the intensity of X-ray reflections and the disappearance of the halo indicate the occurrence of recrystallization processes in the fullerite phase. The absence of X-ray reflections from the titanium crystal lattice is explained by the diffusion of metal atoms into the fullerite matrix and the formation of a new phase of $Ti_xO_yC_{60}$.

Figure 6 shows the AFM images of the signal proportional to the local stiffness of the near-surface

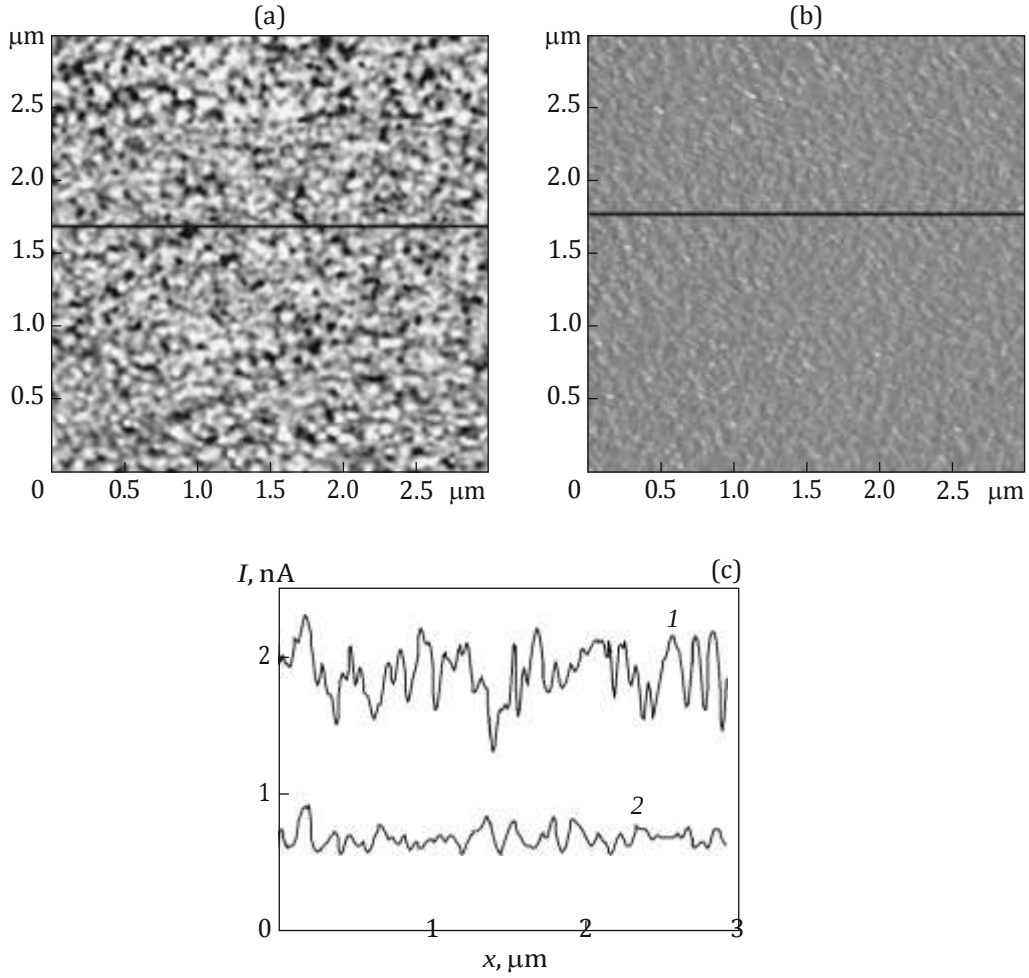

Fig. 6. (a, b) Atomic force microscopy images of the signal proportional to the local stiffness of Ti–C_{60}–Ti films implanted with boron ions and (c) cross-sectional profiles along the selected lines for the films (a, c) before annealing (curve *1*) and (b, c) after annealing at 570 K for 3 h (curve *2*).

region of the films. An analysis of the section profile along the highlighted lines in Fig. 6 showed that the value of the local stiffness at different points on the surface of films implanted with boron ions before annealing differs by a factor of almost 2, whereas the scatter in the values of the signal proportional to the local stiffness is much smaller after annealing (Fig. 6c). The absence of contrast in the AFM image of the annealed films indicates the formation of a single-phase structure with uniform mechanical properties (Fig. 6b). It was found using the nanoindentation method that the dynamic hardness of the implanted films after thermal annealing at 573 K levels off over the entire depth of the film (see Fig. 5, curve *3*), and its value simultaneously increases compared to the nanohardness of unannealed films, which is most likely associated with the annealing of defects and the formation of a new phase of $Ti_xO_yC_{60}$ with improved mechanical properties.

CONCLUSIONS

It is established that intense diffusion of titanium into the fullerite layer occurs during the deposition of a fullerite layer on the underlying titanium layer and then a titanium layer on the fullerite layer. The films have a nanocrystalline structure with an average size of structural components of 40 nm.

Implantation of Ti–C_{60}–Ti films (150–250–120 nm) with boron ions (E = 80 keV, D = 1 × 10^{16} ions/cm^2) leads to an increase in the size of structural components to 60–80 nm, a twofold increase in the oxygen content in the films, the mixing of titanium and fullerite layers, the formation of the $Ti_xO_yC_{60}$ phase, and an increase in the dynamic hardness of the mixed layers. As a result of thermal annealing of Ti–C_{60}–Ti films implanted with boron ions at 570 K (3 h), the growth of a new $Ti_xO_yC_{60}$ phase with improved mechanical properties is observed.

ACKNOWLEDGMENTS

The author thanks V.Ya. Krasnitskii for performing ion implantation of samples and V.A. Ukhov for the elemental analysis of the films by Auger spectroscopy.

CONFLICT OF INTEREST

The author declares that he has no conflicts of interest.

REFERENCES

1. Kopova, I., Lavrentiev, V., Vacik, J., and Bacakova, L., Growth and potential damage of human bone-derived cells cultured on fresh and aged C_{60}/Ti films, *PLoS One*, 2015, vol. 10, no. 4, p. e0123680.
2. Shpilevsky, E.M., Shpilevsky, M.E., Prylutskyy, Y.I., Zakharenko, M.I., and Le Normand, F., Structure and properties of C_{60} fullerene films with titanium atoms, *Materialwiss. Werkstofftech.*, 2011, vol. 42, no. 1, pp. 59–63.
3. Shpilevsky, E.M., Tuvshintur, P., Davaasambuu, Z., Filatov, S.A., and Shilagardi, G., Metal-fullerene materials for electronics, *Nanosci. Technol.*, 2019, vol. 10, no. 4, pp. 303–309.
4. Norin, L., Jansso, U., Dyer, C., Jacobsson, P., and McGinnis, S., On the existence of transition and characterization of Ti_xC_{60}, *Chem. Mater.*, 1998, vol. 10, no. 4, pp. 1184–1190.
5. Nyberg, M., Luo, Y., Qian, L., Rubensson, J.-E., Sathe, C., Ding, D., Guo, J.-H., Kaambre, T., and Nordgren, J., Bond formation in titanium fulleride compounds studied through X-ray emission spectroscopy, *Phys. Rev. B*, 2001, vol. 63, p. 115117.
6. Talyzin, A.V., Jansson, U., Usatov, A.V., Burlakov, V.V., Shur, V.B., and Novikov, Y.N., Comparative Raman study of the Ti complex $Cp_2Ti(\eta^2–C_{60}) \cdot C_6H_5CH_3$ and Ti_xC_{60} films, *Phys. Solid State*, 2002, vol. 44, no. 3, pp. 506–508.
7. Baran, L.V., Shpilevsky, E.M., and Okatova, G.P., Structural-phase transformations in titanium-fullerene films at implantation of boron ions, in *Hydrogen Materials Science and Chemistry of Carbon Nanomaterials*, Veziroglu, T.N., Zaginaichenko, S.Yu., Schur, D.V., Baranowski, B., Shpak, A.P., and Skorokhod, V.V., Eds., Netherlands: Kluwer Academic, 2004, pp. 115–122.
8. Gakhar, T. and Hazra, A., C_{60}-encapsulated TiO_2 nanoparticles for selective and ultrahigh sensitive detection of formaldehyde, *Nanotechnology*, 2021, vol. 32, p. 505505.
9. Vacik, J., Lavrentiev, V., Novotna, K., Bacakova, L., Lisa, V., Vorlicek, V., and Fajgar, R., Fullerene (C_{60})-transitional metal (Ti) composites: Structural and biological properties of the thin films, *Diamond Relat. Mater.*, 2010, vol. 19, no. 2, pp. 242–246.
10. Vandrovcova, M., Vacik, J., Svorcik, V., Slepicka, P., Kasalkova, N., Vorlicek, V., Lavrentiev, V., Vosecek, V., Grausova, L., Lisa, V., and Bacakova, L., Fullerene C_{60} and hybrid C_{60}/Ti films as substrates for adhesion and growth of bone cells, *Phys. Status Solidi A*, 2008, vol. 205, pp. 2252–2261.
11. Talyzin, A.V. and Jansson, U., A comparative Raman study of some transition metal fullerides, *Thin Solid Films*, 2003, vol. 429, nos. 1–2, pp. 96–101.
12. Afreen, S., Muthoosamy, K., Manickam, S., and Hashim, U., Functionalized fullerene (C_{60}) as a potential nanomediator in the fabrication of highly sensitive biosensors, *Biosens. Bioelectron.*, 2015, vol. 63, pp. 354–364.
13. Anila, S. and Suresh, C.H., Endo- and exohedral chloro-fulleride as η^5 ligands: A DFT study on the first-row transition metal complexes, *Phys. Chem. Chem. Phys.*, 2021, vol. 23, no. 5, pp. 3646–3655.
14. Makarets, M.V., Prylutskyy, Yu.I., Zaloyilo, O.V., and Scharff, P., Fragmentation of free and supported C_{60} fullerenes by ion beam, *Fullerenes*, *Nanotubes*, *Carbon Nanostruct.*, 2005, vol. 13, pp. 339–346.

15. Baran, L.V., Structure-phase state, electric and mechanical properties of fullerite films implanted with boron ions, *Fiz. Khim. Obrab. Mater.*, 2008, no. 4, pp. 18–22.
16. Dall'Asén, A.G., Verdier, M., Huck, H., Halac, E.B., and Reinoso, M., Nanoindentation on carbon thin films obtained from a C_{60} ion beam, *Appl. Surf. Sci.*, 2006, vol. 252, pp. 8005–8009.
17. Todorović-Marković, B., Draganić, I., Vasiljević-Radović, D., Romčević, N., Romčević, M., Dramićanin, M., and Markovic, Z., Synthesis of amorphous boron carbide by single and multiple charged boron ions bombardment of fullerene thin films, *Appl. Surface Sci.*, 2006, vol. 144, nos. 1–4, pp. 75–81.
18. Sharma, P., Singhal, R., Vishnoi, R., Agarwal, D.C., Banerjee, M.K., Chand, S., Kanjilal, D., and Avasthi, D.K., Effect of Ag ion implantation on SPR of Cu–C_{60} nanocomposite thin film, *Plasmonics*, 2018, vol. 13, pp. 669–679.
19. Baran, L.V., Effect of boron ion implantation on the structure, phase composition, and mechanical properties of chromium-fullerite-chromium films, *Inorg. Mater.: Appl. Res.*, 2018, vol. 3, pp. 370–375. https://doi.org/10.1134/S2075113318030061
20. http://www.srim.org
21. Baran, L.V., Annealing effect on the structure, phase composition, and nanohardness of titanium/fullerite films, *Inorg. Mater.*, 2010, vol. 46, no. 8, pp. 824–832.
22. Chen, J., Xu, J.B., Xue, K., An, J., Ke, N., Cao, W., Xia, H.B., Shi, J., and Tian, D.C., Nanoscale structural characteristics and electron field emission properties of transition metal–fullerene compound TiC_{60} films, *Microelectron. Reliab.*, 2005, vol. 45, no. 1, pp. 137–142.
23. Wang, W.H. and Wang, W.K., Interactions between the interface of titanium and fullerene, *J. Appl. Phys.*, 1996, vol. 79, no. 1, pp. 149–152.
24. Fomenko, L.S., Lubenets, S.V., Sidorov, N.S., Osip'yan, Yu.A., Orlov, V.I., and Izotov, A.N., Dislocation mobility in C_{60} fullerite crystals, *Phys. Solid State*, 2007, vol. 49, pp. 800–804.
25. Richter, A., Ries, R., Smith, R., Henkel, M., and Wolf, B., Nanoindentation of diamond, graphite and fullerene films, *Diamond Relat. Mater.*, 2000, vol. 9, no. 2, pp. 170–184.